High-Resolution Reconstruction for NoData Gaps in Narrow Angle Camera Digital Terrain Models using Gaussian Process-Latent Variable Model. Y. J. Park[1], S. H. Moon[2], and H. L. Choi[3], Department of Aersopace Engineering, Korea Advanced Institute of Science and Technology (KAIST), 291 Daehak-ro, Yuseong-gu, 34141, Daejeon, Republic of Korea ([1]yjpark@lics.kaist.ac.kr, [2]shmoon@lics.kaist.ac.kr, [3]hanlimc@kaist.ac.kr).

Introduction: With the advent of NASA's lunar reconnaissance orbiter (LRO) [1, 2], a large amount of data has been collected to characterize the moon's surface. One of the most important roles of LRO is to identify elevations of lunar surface and construct the digital terrain models (DTMs) by using data obtained from the lunar orbiter laser altimeter (LOLA) measures and the Lunar Reconnaissance Orbiter Camera (LROC). Although LOLA provides a global topographic model, LOLA-only DTMs only have 1024 pixel per degree (~30m at the equator) resolution. On the other hand, LROC can construct high-resolution (~5m at the equation) local DTMs by using stereo data from two narrow angle cameras (NACs) [3]. However, during the stereo-matching process, NAC DTMs often have NoData gap regions due to the shadows. Existing approaches often filled those gaps using low-resolution LOLA data [4] or interpolation, but we suggest improved data-driven approach to reconstruct gaps in NAC DTMs preserving high-resolution by using Gaussian process latent variable model (GP-LVM). We also suggest optimization approach to further improve reconstructed DTMs' quality.

Data Set: We applied proposed method onto two adjacent 250px×250px (1.25km×1.25km) DTMs (y^*) near Apollo 17 landing site (20.0°N and 30.4°E). The NoData gaps (y_u^*) are 11890 pixels (~ 0.3 km^2). The training data (Y) of NAC DTMs are obtained near the target region (19.8-20.1°N and 30.2-30.6°E; Fig. 1).

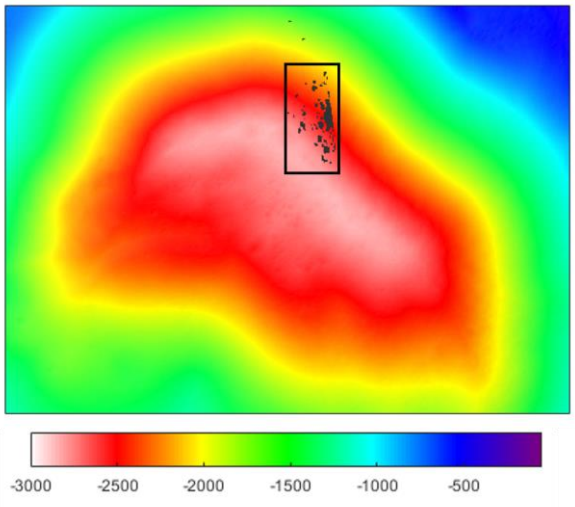

Figure 1. DTMs used for training data. Squared region is test region to be reconstructed.

By rotating training DTMs, data augmentation has been done to retain a variety of data set and improve reconstruction accuracy. Total 182108 training data are initially generated. LROC images used for training and test data are at wms.lroc.asu.edu/lroc.

Algorithms: GP-LVM is unsupervised learning approach using Gaussian process (GP) suggested by [5]. GP-LVM has been widely used to design probabilistic mapping between high-dimensional data and lower-dimensional latent space (X). GP-LVM is formulated as:

$$\mathrm{p(Y|X)} = \prod_{d=1}^{D} N(y_d|0, K_{NN} + \beta^{-1} I_N) \qquad (1)$$

where $\mathrm{y_d}$ is dth dimension values of Y and $K_{NN} + \beta^{-1} I_N$ is GP covariance matrix among latent space. GP covariance matrix is often designed by automatic relevance determination (ARD) squared exponential (SE) kernel function:

$$\mathrm{K}(x, x') = \sigma_0^2 \exp\left(-\frac{1}{2}\sum_d \left(\frac{x_d - x'_d}{\lambda_d}\right)^2\right) \qquad (2)$$

where σ_0 and λ_d are kernel hyperparameters that GP-LVM should learn. GP-LVM can be trained by maximizing the variational lower bound of the model for given training data. Since derivatives of the lower bound for each hyperparameter are analytically tractable, scaled conjugated gradient method is used for optimization in this work.

For any given test DTMs with NoData gaps, we can find the optimal vector x^* in the latent space that represents observed components ($y_o^* = y^* - y_u^*$) by maximizing approximate marginal likelihood $\mathrm{p}(y_o^*|Y)$. Then, by using GP-LVM and multi-variate normal theory, probabilistic reconstruction of NoData gaps in NAC DTMs is achieved. The reconstruction results are shown in Fig. 2.

GP-LVM only approach does not guarantee to reconstruct continuous DTMs along the contour of gaps. To solve the problem, the optimization technique is applied considering two aspects: (1) final reconstruction values should be close to the output from GP-LVM as much as possible, and (2) elevation values in DTMs should be continuous (i.e. there are upper bounds for absolute values of the derivatives). Finally, we optimize reconstructed DTMs through following linearly constrained quadratic programming with linear constraints for reconstructed regions:

$$y_u^* = \underset{y}{\operatorname{argmin}} \sum_{i,j} \left\| y_{i,j} - y_{i,j}^{GPLVM} \right\| \quad s.t. \qquad (3)$$
$$\left| y_{i-1,j} - y_{i+1,j} \right|, \quad \left| y_{i,j-1} - y_{i,j+1} \right| \le U_{i,j}^{(1)}$$
$$\left| y_{i-1,j} - 2y_{i,j} + y_{i+1,j} \right|, \quad \left| y_{i,j-1} - 2y_{i,j} + y_{i,j+1} \right| \le U_{i,j}^{(2)}$$

where $U^{(1)}$ and $U^{(2)}$ are upper bounds for first and second derivatives, respectively. Upper bounds can be arbitrarily selected by user experience. In fact, selecting proper values are also additional topic to be studied. In this work, we determined the value as the maximum derivative values around the test region. Overall algorithm flow is as illustrated in Algorithm 1. The comparison between GP-LVM only and optimized reconstruction results are as shown in Fig. 3, representing smoother reconstructions for NAC DTMs.

Alogorithm 1. Reconstructions of NAC DTM	
1:	Choose [a] N samples among Y. Let them Y_N.
2:	Train GP-LVM with Y_N.
3:	Find x^* maximizing $p(y_o^*|x^*)$ by GP-LVM.
4:	Reconstruction NAC DTMs with output y_u^* mapped from x^* via GP-LVM.
5:	Optimize reconstructions by (3).

a) Samples are often chosen by neighborhoods of test data, y^*.

Conclusion: High-resolution reconstruction approach for NoData Gaps in NAC DTMs was proposed by using GP-LVM. Suggested reconstruction method still preserves high-resolution of original NAC DTMs. Quality of reconstructed regions in NAC DTMs were further improved by optimization restricting the first and second order derivative values.

In future, more accurate machine learning models such as deep Gaussian processes can be applied. Another interesting topic is to suggest more sophisticated optimization formulation by integrating LOLA DTMs as well.

References: [1] Chin, et al. (2007) Space Sci. Rev., 129, 391-419. [2] Smith, et al. (2010) Space Sci. Rev., 150, 209-241. [3] Tran, T., et al. (2010) ASPRS/CaGIS Specialty Conference. [4] Gläser, P., et al. (2013) LPSC 44, #1967. [5] Titsias, et al. (2010) AISTATS 13, p. 844-851.

Acknowledgement: This research was prepared at the Korea Advanced Institute of Science and Technology (KAIST), Department of Aerospace Engineering under a research grant from the National Research Foundation of Korea (NRF-2016M1A3A3A02017919).

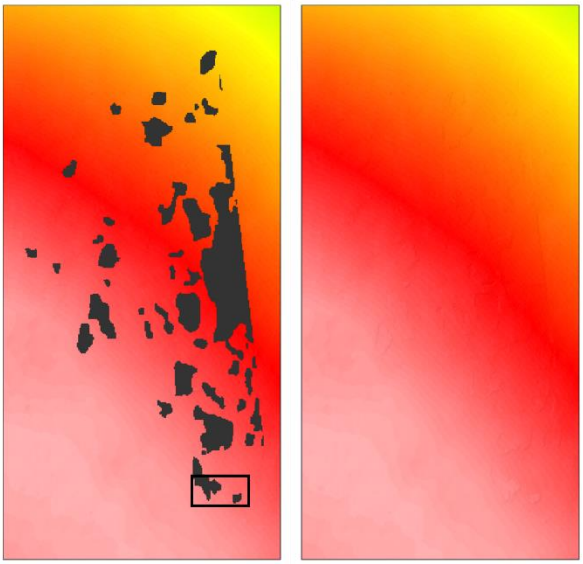

Figure 2. Reconstruction via GP-LVM. Squared region is shown in Fig. 3.

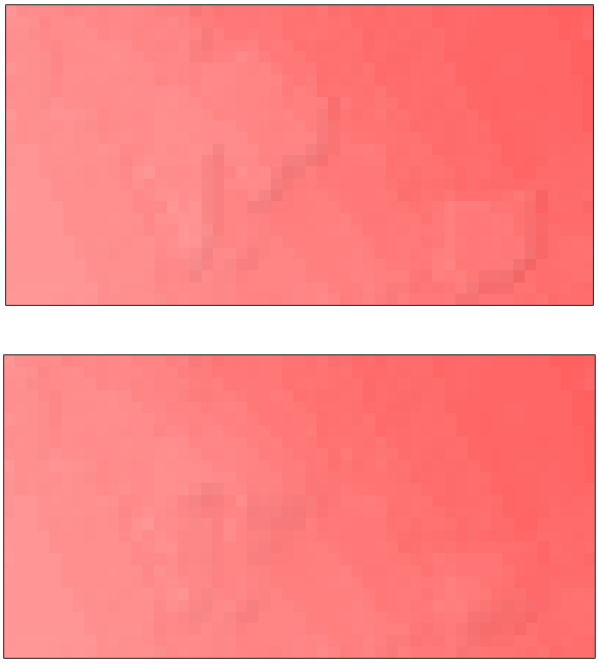

Figure 3. Improvement via optimization. The top image is a GP-LVM only reconstruction result, while the bottom is a result of optimization.